*Progress In Electromagnetics Research, PIER 8, 349–375, 1994*

# FAST AND ACCURATE INTERPOLATION OF RADIATED FIELDS OVER A CYLINDER

*C. Gennarelli, G. Riccio, C. Savarese, and V. Speranza*



## 1. Introduction

Besides the well-known applications to communications and signal processing, the use of sampling expansions has proved to be of wide applicability also in the Near Field-Far Field (NF-FF) transformation techniques [1–5] as well as in an efficient antenna pattern evaluation [6–10]. This fact relies for its mathematical justification on the properties of scattered or radiated electromagnetic fields, which can be closely approximated by spatially bandlimited functions. Such a bandwidth depends only on the overall dimension of the radiating system [11]. Accordingly, the Cardinal Series (CS) expansions seem to be the appropriate tools for a convenient representation of the electromagnetic field.

These standard expansions, however, have the drawback that, to keep the truncation error low, all the relevant samples must be considered when evaluating the field at each output point and this would lead to unacceptably large computational times. Furthermore, due to the slow decay of the CS functions, the errors affecting the data propagate

from high to low field regions giving rise to large relative errors in the latter ones.

To overcome these problems, in [5, 10, 12, 13] have been proposed the use of more efficient sampling expansions of central type, which minimize the truncation error for a given number of retained samples. In particular the papers [5] and [13] deal with the electromagnetic field interpolation in the plane-polar geometry, [10] refers to the spherical case, and [12] is concerned with the plane-rectangular one.

This paper is devoted to the development of efficient sampling interpolation algorithms of central type which allow the accurate reconstruction of scattered or radiated fields over a cylindrical surface from a minimum number of samples. To this end, various sampling expansions are here developed and compared in order to determine the optimal one.

This problem is relevant not only in NF-FF transformation with cylindrical scanning, but also whenever an efficient reconstruction of the electromagnetic field over a cylinder is wanted, and can be of a some relevance in other areas, such as X-ray Tomography [14, 15] and Nuclear Magnetic Resonance [16].

A summary of previous results concerning the sampling interpolation of a bandlimited function on a rectilinear and on a circular domain are briefly referred in Section 2. Two-dimensional sampling expansions of central type relevant to a cylindrical domain are derived in Section 3 and applied to the reconstruction of electromagnetic radiated fields. In Section 4 the proposed techniques are tested by means of some numerical simulations of pattern reconstruction from both field and power samples. Moreover, in the same Section, the reconstruction error plots are presented and compared with the theoretical upper bounds derived in Section 3. The algorithm stability with respect to both absolute and relative measurements errors, which unavoidably affect the data, is proved in Section 5 by adding randomly distributed errors to the ideal samples. Conclusions are collected in Section 6.

## 2. Summary of Optimal One-Dimensional Sampling Series

Let us consider the most general linear approximation scheme of a bandlimited function $F$ from uniformly distributed samples, centered

on the output point $s$ :

$$\tilde{F}(s) = \sum_{m=-p+1}^{p} F(s_m)\, G_m(s) \tag{1}$$

where $2p$ is the number of retained samples, $s_m = m\Delta s$ are the sampling point positions, $\{G_m\}$ is the set of approximating functions and, with no loss of generality, the output point is assumed to lie in the interval $[0, \Delta s]$.

Then the following question naturally arises: given the bandwidth $w$, the sample spacing $\Delta s$, and the number $2p$ of retained samples, determine the set $G_m$ which minimizes the maximum normalized error

$$\delta = \varepsilon(F/\|F\|) = \frac{1}{\|F\|} \sup_{0 \le s \le \Delta s} |\tilde{F}(s) - F(s)| \tag{2}$$

where

$$\|F\| = \sup_{s} |F(s)| \tag{3}$$

is the uniform norm of $F$.

The solution to this problem, for the functions belonging to the set $E_w$ of square integrable functions bandlimited to $w$, has been known for a long time and it is briefly referred to in [12]. A similar solution for the functions belonging to the set $B_w$ of bounded functions, bandlimited to $w$, has been obtained recently [17]. For both the cases, the resulting scheme is of interpolatory type, since the optimal functions satisfy the conditions:

$$G_m(n\Delta s) = \delta_{mn}; \qquad m, n = -p+1, \ldots, p \tag{4}$$

wherein $\delta_{mn}$ is the Kroenecker symbol.

However, these algorithms are not user friendly; the approximating functions change with the number of the samples and generally cannot be evaluated in a closed form.

Fortunately, there have been found substitutes practically optimal for these unmanageable optimal functions. By using these practically optimal functions, the expression (1), in the case of the interpolation over a rectilinear domain, becomes

$$\widetilde{F}(s) = \sum_{m=-p+1}^{p} F(s_m)\, \Psi(s - s_m)\, \mathrm{sinc}\left[\frac{\pi}{\Delta s}(s - s_m)\right] \tag{5}$$

where $\mathrm{sinc}(s)$ is the $\sin(s)/s$ function and $\Psi(s)$ is a convergence factor.

If $F \in B_w$, the proper convergence factor [12] is the Approximate Prolate Spheroidal (APS) function:

$$P(s) = \frac{\sinh\left[\pi\nu p\sqrt{1 - \left(\dfrac{s}{p\Delta s}\right)^2}\right]}{\sinh(\pi\nu p)\sqrt{1 - \left(\dfrac{s}{p\Delta s}\right)^2}}; \qquad \nu = \left(1 - \frac{1}{\chi}\right) \tag{6}$$

first introduced by Knab [18]. In (6) $\chi = \pi/w\Delta s > 1$ is the oversampling factor, i.e., the ratio between the actual sampling rate $1/\Delta s$ and the Nyquist one, $w/\pi$.

Analogously, in the case of a function $F \in E_w$, the practically optimal choice [12] for $\Psi(s)$ is provided by the Sampling Window ($SW$) function:

$$Q(s) = \frac{\cosh\left[\pi\nu p\sqrt{1 - \left(\dfrac{s}{p\Delta s}\right)^2}\right]}{\cosh(\pi\nu p)} \tag{7}$$

also introduced by Knab [19].

A simple upper bound of the truncation error for the APS series is [18]:

$$\delta < \frac{1}{\sinh(\pi\nu p)} \tag{8}$$

An analogous upper bound for the SW series has not yet been found, only bounds in terms of the square norm of $F$ being available [12, 19].

The truncation error upper bounds for these expansions have been compared in [12] with the corresponding bounds for the optimal ones and it has been found that the performance differences are

small. Therefore, in any practical application, the Knab expansions are the natural and convenient substitutes for the cumbersome optimal functions.

Let us now turn to the case of the interpolation over a circumference. In such a case, since the domain is closed, the results are $B_w \equiv E_w \equiv P_M, P_M$ being the space of trigonometric polynomials of (maximum) degree equal to $M$.

The analog of (5) then becomes [10]:

$$\widetilde{F}(\phi) = \sum_{m=-p+1}^{p} F(\phi_m)\, \Phi(\phi - \phi_m)\, D_{M'}(\phi - \phi_m) \tag{9}$$

wherein $\phi_m = m\Delta\phi$ and the output point is assumed to lie in the angular interval $[0, \Delta\phi]$. In (9)

$$D_{M'}(\phi) = \frac{\sin\left(\dfrac{2M'+1}{2}\,\phi\right)}{(2M'+1)\,\sin(\phi/2)} \tag{10}$$

is the Dirichlet function and

$$M' = \mathrm{Int}\,(\chi M) + 1 \tag{11}$$

$\mathrm{Int}(x)$ denoting the greatest integer less than or equal to $x$.

The proper convergence factor $\Phi$ is either the so called Discrete Approximate Prolate Spheroidal (DAPS) function:

$$S_N(\phi, \phi_0) = \frac{\sinh\left[(2N+1)\sinh^{-1}\sqrt{\sin^2(\phi_0/2) - \sin^2(\phi/2)}\right]\sin(\phi_0/2)}{\sinh\left[(2N+1)\sinh^{-1}(\sin(\phi_0/2))\right]\sqrt{\sin^2(\phi_0/2) - \sin^2(\phi/2)}} \tag{12}$$

or the Tschebysceff Sampling (TS) one:

$$\Omega_N(\phi, \phi_0) = \frac{T_N\left[2\left(\dfrac{\cos(\phi/2)}{\cos(\phi_0/2)}\right)^2 - 1\right]}{T_N\left[\dfrac{2}{\cos^2(\phi_0/2)} - 1\right]} \tag{13}$$

wherein $\phi_0 = p\Delta\phi$, and $T_N(\cdot)$ is the Tschebysceff polynomial of degree $N = M' - M$.

The convergence factors $S_N$ and $\Omega_N$ have been obtained [10] by paralleling the properties of the APS and SW functions, respectively. Accordingly, it can be expected that DAPS series expansion should be more suitable to represent flat functions, whereas the TS one should be more appropriate for those which exhibit a "concentrated" pattern. A truncation error upper bound for the DAPS series is [20]:

$$\delta < \frac{2}{\pi \sinh(\pi\nu p)} \left[ (\pi\nu p) \ln \sqrt{1 + \frac{1}{(\pi\nu p)^2}} + \tan^{-1}(\pi\nu p) \right]$$
$$\lesssim \frac{1}{\sinh(\pi\nu p)} \tag{14}$$

and for the TS one [20] :

$$\delta < \frac{2}{\pi T_N[2/\cos^2(\phi_0/2) - 1]} \ln \left[ \cot\left( \frac{p\pi}{4M'} \right) \right]$$
$$\underset{p/M \ll 1}{\cong} \frac{2}{\pi} \frac{\ln\left( \frac{4\chi M}{\pi p} \right)}{\cosh(\pi\nu p)} \tag{15}$$

Such central type series provide a fully satisfactory answer to the problem of controlling the truncation error in a practically optimal way.

## 3. Optimal Interpolation over a Cylinder

Let us consider the electric field $\underline{E}(\underline{r})$ radiated by a source $S$ and a cylindrical observation domain (see Fig. 1). If the phase propagation factor $\exp(-j\beta r)$ is singled out from the expression of $\underline{E}(\underline{r})$ and an appropriate set of coordinates is used on the observation domain, the new function so obtained

$$\underline{F}(\underline{r}) = \underline{E}(\underline{r}) \exp(j\beta r) \tag{16}$$

still referred to in the following as the radiated field, can be well approximated by spatially bandlimited functions [11]. Such a bandwidth is related to overall dimension of the source and is practically equal to $\beta a$, where $a$ is the radius of the (smallest) ball enclosing the radiating system. As a consequence, the field can be represented by a bandlimited function characterized by a (spatial) bandwidth $w = \chi'\beta a$. The enlargement bandwidth factor $\chi'$ allows control of the bandlimitation error [11].

The required reconstruction formula of electromagnetic fields over a cylinder of radius $d$ from uniformly spaced samples can be easily obtained by matching together the previously referred sampling expansions for a rectilinear and a circular domain.

Accordingly, by assuming $s = z/d$, we get for each field component:

$$\tilde{F}(s,\phi) = \sum_{n=n_0-q+1}^{n_0+q} \left\{ \Psi(s-s_n)\ \mathrm{sinc}\left[\frac{\pi}{\Delta s}(s-s_n)\right] \cdot \sum_{m=m_0-p+1}^{m_0+p} \Phi(\phi-\phi_{n,m})\, D_{M'_n}(\phi-\phi_{n,m})\, F(s_n,\phi_{n,m}) \right\} \quad (17)$$

where

$$s_n = n\Delta s = \frac{n\pi}{\chi'\chi\beta a}, \qquad \phi_{n,m} = m\Delta\phi_n = \frac{2\pi m}{(2M'_n+1)} \quad (18)$$

$$M'_n = \mathrm{Int}\,(\chi M_n) + 1 \quad (19)$$

$$M_n = \mathrm{Int}\,(\chi^*\beta a \sin\theta_n) + 1, \qquad \tan\theta_n = \frac{1}{s_n} \quad (20)$$

and $n_0 = \mathrm{Int}(s/\Delta s), m_0 = \mathrm{Int}(\phi/\Delta\phi_0)$ are the indexes of the sample nearest (on the left) to the output point. The number of the retained samples along $s$ and $\phi$ is $2q$ and $2p$, respectively. In (20), the azimuthal excess bandwidth factor $\chi^*$ is

$$\chi^* = \chi^*(\theta) = 1 + (\chi' - 1)\,(\sin\theta)^{-2/3} \quad (21)$$

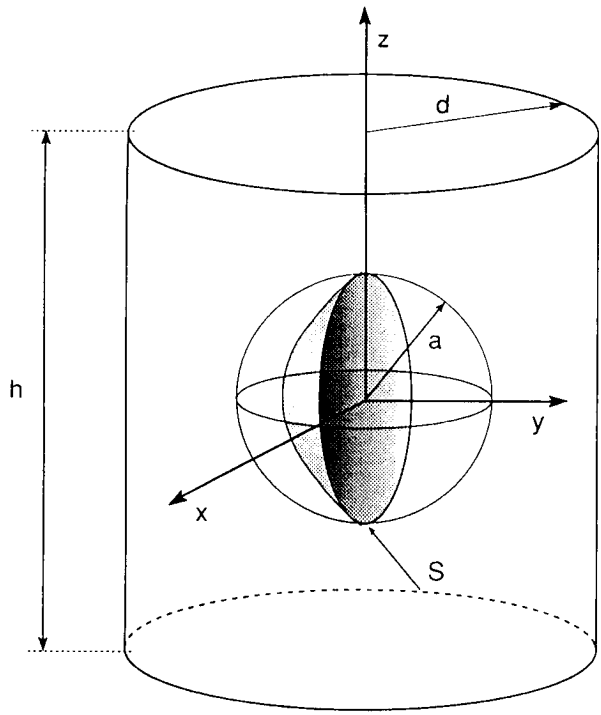


**Figure 1. Relevant to a cylindrical observation domain.**

and the variation with $\theta$ is required to ensure a bandlimitation error constant with respect to $s$ [11].

It is noteworthy that, as a straightforward consequence of the frequency convolution theorem, the squared amplitude of the field is an almost bandlimited function with bandwidth $2w$. Accordingly, the expansion (17) can be applied to any squared amplitude field component, provided that the sampling spacings are halved.

Explicit truncation error upper bounds relevant to the different possible choices for the weight functions in (17) are derived in the Appendix, both by using the uniform norm and the square one.

For the maximum normalized error, it results in the uniform norm:

$$\delta_{pq} = \frac{\varepsilon_{pq}}{\|F\|} \leq (1+\delta_p)(1+\delta_q) - 1 \cong \delta_p + \delta_q \qquad (22)$$

and in the square one:

$$\delta_{pq} = \frac{|\varepsilon_{pq}|}{\|F\|} \leq \sqrt{2\pi H}\chi'\chi\left(\frac{2a}{\lambda}\right)\sqrt{\bar{\delta}_p^2 + \bar{\delta}_q^2} \tag{23}$$

The relation (22) shows that, as in the case of the plane-rectangular [12], spherical [10], and plane-polar [13] geometries, the error upper bound, obtained by using the uniform norm, can be expressed in terms of the one-dimensional bounds $\delta_p$ and $\delta_q$.

In (23) the quantities $\bar{\delta}_q^2, \bar{\delta}_p^2$, as well as the normalized equivalent height $H$ of the field distribution over the cylinder, are defined in the Appendix.

Explicit upper bounds for $\bar{\delta}_p^2$ have been derived in [20], where it is shown that:

$$\bar{\delta}_p^2 \underset{\substack{p/M' \ll 1 \\ N \gg 1}}{\leq} \frac{2}{\pi} \frac{\nu}{\sinh^2(\pi\nu p)} \frac{\ln\left(\sqrt{1+(\pi\nu p)^2} + \pi\nu p\right)}{\pi\nu p} \tag{24}$$

for the DAPS expansion and:

$$\bar{\delta}_p^2 \underset{p/M' \ll 1}{<} \frac{2}{p\pi^2 \cosh^2(\pi\nu p)} \tag{25}$$

for the TS one.

The upper bounds for $\bar{\delta}_q^2$ are derived in [12] for the APS series and in [19] for the SW one. They read respectively:

$$\bar{\delta}_q^2 < \frac{\ln[(2q+1)(q+1)]}{2q\pi^2 \sinh^2(\pi\nu q)} \tag{26}$$

$$\bar{\delta}_q^2 < \frac{2}{\pi^2 \cosh^2(\pi\nu q)} \frac{4q}{4q^2 - 1} \tag{27}$$

It is worthy to note that the bound (23) can be tighter than (22) when the field is focused and is the only one available when the SW series, which lacks a uniform one-dimensional bound, is used.

## 4. Numerical Tests

Many numerical tests have been carried out in order to assess the effectiveness of the proposed algorithm and to give a heuristic response to the problem of the optimal choice for the azimuthal and rectilinear sampling functions. This section deals with the interpolation of electromagnetic radiated fields from ideal samples, whereas the reconstruction from real (i.e. error affected) data is explicitly considered in the next section.

The examples, reported in the following, are relevant to the electric field radiated by a non-focusing planar circular array (see Fig. 2). The array diameter $2a$ is $24\lambda$, its elements are $0.6\lambda$ spaced along the radii and along the rings and are assumed to be elementary Huygens sources linearly polarized along the $z$ axis. Only 20% of them, randomly distributed, are active (Fig. 3). The excitation amplitudes have been chosen tapered with respect to the $z$ and $x$ axis with a $\cos^2$ law. The phases are the superposition of a random term, uniformly distributed in the range $(-\pi/2, \pi/2)$, and a $x$-dependent cubic one. This makes the radiated field highly variable, giving rise to severe reconstruction conditions. Moreover, it has been assumed that the array is symmetric and symmetrically excited with respect to the $x$ axis.

The height and the radius of the cylindrical zone covered by the samples are $60\lambda$ and $18\lambda$, respectively.

In order to select the value of the enlargement bandwidth factor $\chi'$ which, as previously stated, allows the control of the aliasing error, the actual mean-square and maximum normalized errors have been evaluated by reconstructing the field with the CS expansion. These errors have been evaluated by comparing the reconstructed and the exact $z$-component of the field (the most significant one) on a cylindrical grid with a linear step $\Delta z = 0.316\lambda$, and an azimuthal one $\Delta\phi = 1°$.

Note that, in order to lower significantly the unavoidable truncation error relevant to the sampling along $z$, the evaluation has been performed on a reduced cylinder having a 60% height of the initial one.

The results are collected in Table 1, where the mean square and maximum normalized errors, relevant to various $\chi'$ values, are reported together with the overall number of the corresponding samples.

As expected, on increasing $\chi'$, the errors decrease quite rapidly until very low levels are reached. This behaviour is, obviously, due to the residual influence of the truncation in the sampling along $z$.

According to the data reported in Table 1, in the following, $\chi'$ has been chosen equal to 1.20, which practically corresponds to the errors saturation.

The maximum and mean-square normalized errors, relevant to the different choices for the central sampling functions, have been computed over the above reduced zone by assuming, for simplicity, an equal number of retained samples both along $z$ and $\phi$, i.e., $2q = 2p$. This allows to compare quantitatively the possible alternatives for the azimuthal and rectilinear sampling weight functions. The results are collected as curve families, with $\chi$ as ordinate and $p$ as abscissa. On the same plots, the theoretical upper bounds of the truncation error, as well as the actual errors, relevant to the CS truncated to the same number of samples, have also been reported for reference.

The maximum errors for the APS + DAPS case and the APS + TS one are plotted in Fig. 4 and Fig. 5, respectively. By the light of the showed results, the TS weight function for the azimuthal sampling is better than the DAPS one. As it is clearly shown in Fig. 6, even better results can be obtained by using the SW function for the sampling along $z$. Accordingly, the choice of the SW+TS expansion is just the one minimizing the errors for given $\chi$ and $p$ values.

It is worthy to note that the error curves, relative to the CS truncated to the same $p$, are practically independent from $\chi$ and considerably higher than those relevant to the proposed algorithms. Moreover, the actual errors are remarkably lower than the theoretical ones: $\approx 30$ dB for the APS+DAPS and APS+TS cases, $\approx 40$ dB for the SW+TS one. This is not surprising since the theoretical results, being upper bounds, are generally pessimistic.

Two representative interpolation examples, relevant to the SW + TS expansion, are reported in Figs. 7 and 8. They show the amplitude of the field $z$-component, along two cylinder generatrices at $\phi = 90°$ and $\phi = 30°$. As it can be seen, notwithstanding the moderate $\chi$ value and the few retained samples, the pattern reconstruction is very accurate.

As it has been explicitly pointed out in Section 3, the proposed algorithms allow to reconstruct the squared module of the field from power samples. A demonstrative reconstruction example, relevant to the same situation of Fig. 7, is shown in Fig. 9.

| $\chi'$ | Mean square error (dB) | Maximum error (dB) | Number of samples |
|---|---|---|---|
| 1.05 | -67.3 | -52.7 | 10921 |
| 1.10 | -75.1 | -60.8 | 12051 |
| 1.15 | -79.9 | -63.3 | 13255 |
| 1.20 | -81.5 | -65.4 | 14491 |
| 1.25 | -82.1 | -63.8 | 15807 |
| 1.30 | -82.3 | -64.8 | 17119 |

**Table 1.**

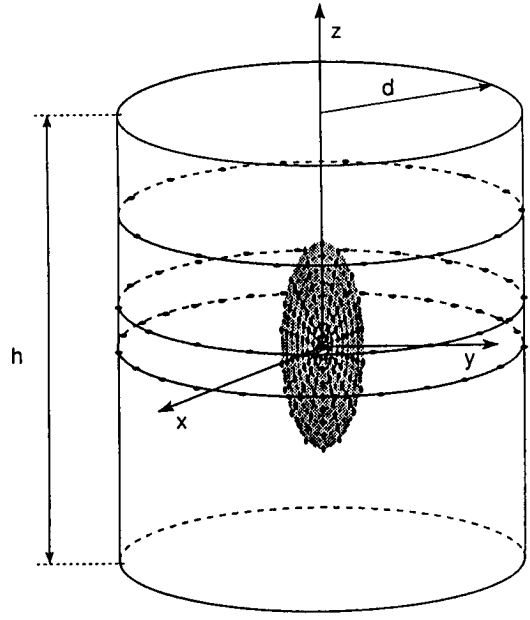


**Figure 2. Geometry of the numerical examples.**

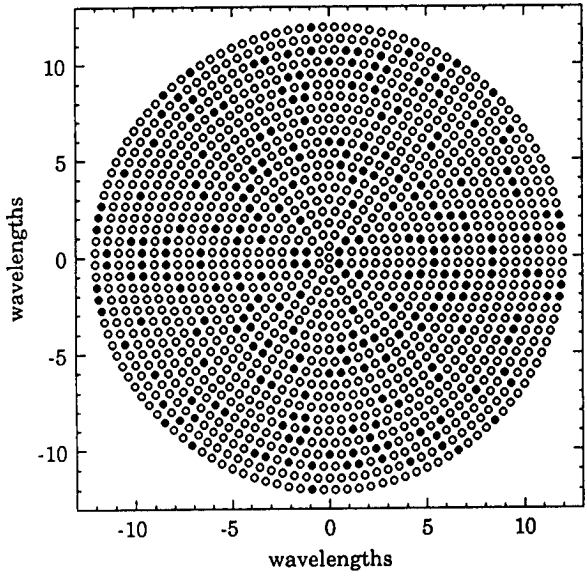


**Figure 3. Active elements layout.**

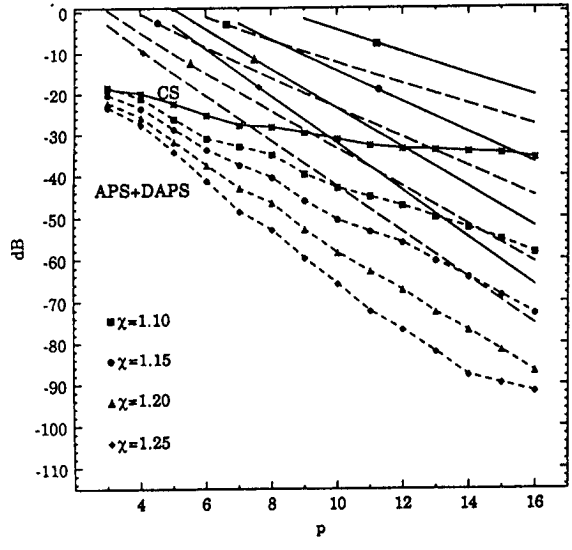


**Figure 4. Maximum reconstruction error for the APS + DAPS series. Field $z$-component. Solid line: square norm theoretical upper bound. Dashed line: uniform norm theoretical upper bound.**

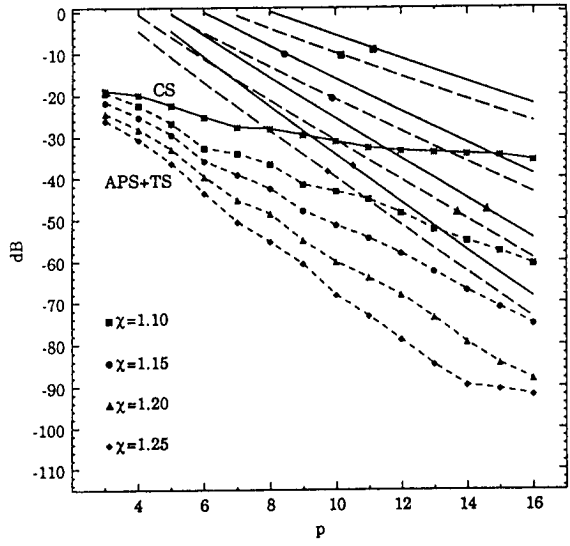


Figure 5. Maximum reconstruction error for the APS + TS series. Field $z$-component. Solid line: square norm theoretical upper bound. Dashed line: uniform norm theoretical upper bound.

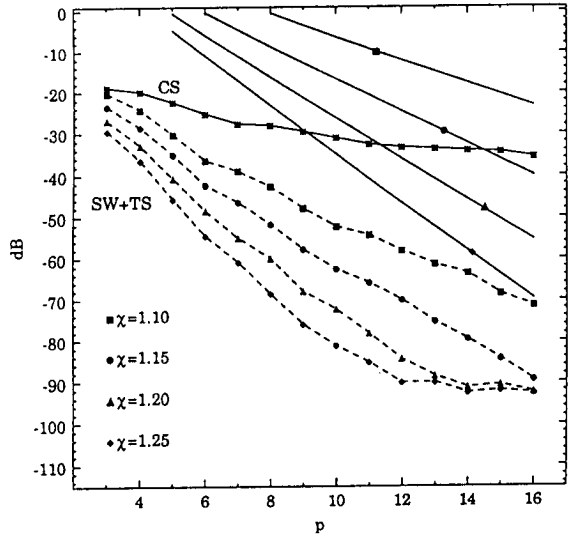


Figure 6. Maximum reconstruction error for the SW + TS series. Field $z$-component. Solid line: square norm theoretical upper bound.

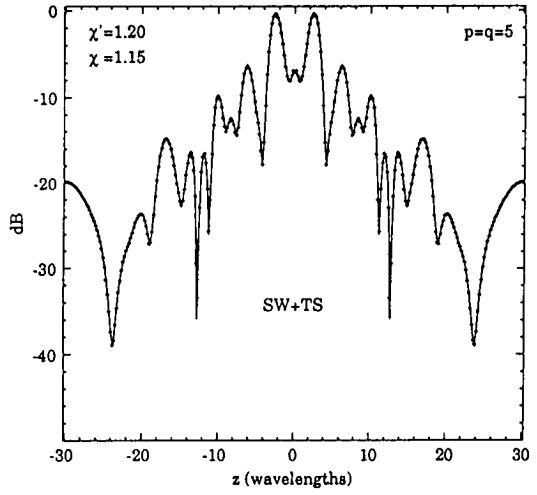


**Figure 7. Amplitude of the field $z$-component on a cylinder line at $\phi = 90°$. Solid line: exact field. Crosses: interpolated by the SW + TS expansion.**

## 5. Algorithm Stability

This section deals with the algorithm stability, i.e., the feature that small errors in sample values give rise to small errors in the reconstruction of the function. This is a mandatory requirement for the interpolation from non-ideal samples, since measured data are unavoidably affected by inaccuracies.

The stability of the sampling expansions has been explicitly considered in [5], where it has been shown that the central sampling series is stable with respect to both absolute and relative errors, while the CS is stable only with respect to the absolute ones.

To assess the stability of the developed algorithm, many numerical tests have been carried out by adding uniformly distributed random errors to the field samples. We have assumed that the data are affected by a background noise (bounded to $\Delta a$ dB in amplitude) and that each sample is known with an uncertainty of $\pm\Delta a_r$ dB in amplitude and $\pm\Delta\phi$ degrees in phase.

A typical reconstruction example from error affected samples, which shows the different behaviour of the SW + TS expansion and

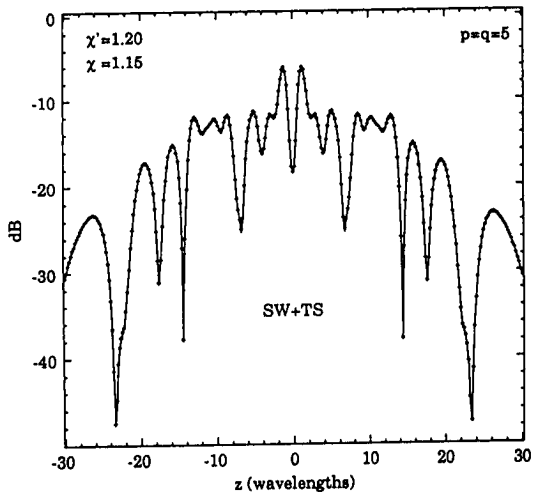


**Figure 8. Amplitude of the field $z$-component on a cylinder generatrix at $\phi = 30°$. Solid line: exact field. Crosses: interpolated by the SW + TS expansion.**

of the CS one, is reported in Fig. 10. It refers to the same situation of Fig. 7, but starting from samples known with uncertainties $\Delta a_r = 0.5$ dB and $\Delta\phi = 10°$.

As it can be seen, the reconstruction obtained with the SW + TS series is more accurate than that relevant to the CS. This different behaviour is due to the slow decay of the CS functions, which causes the propagation of the errors from the strong field regions to the lower field ones giving rise to a strong relative error in the latter.

It can be expected that this different behaviour would be enhanced when interpolating fields characterized by larger dynamics. This is clearly confirmed by the following Fig. 11, where a reconstruction example is reported on a cylinder ring at $z = 26\lambda$ relevant to a new source of the same size of the previous one, but with a high tapering degree. Note that, to test the algorithm in severe reconstruction conditions, the chosen ring is relative to a low field zone and we have assumed that the samples are affected also by a background noise of $-60$ dB.

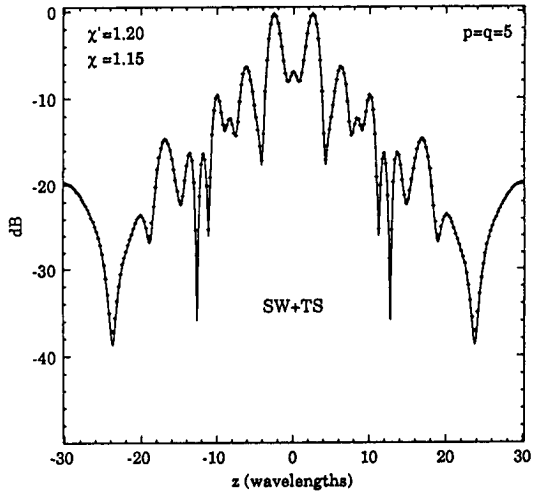


**Figure 9. Amplitude of the field $z$-component on a cylinder generatrix at $\phi = 90°$. Solid line: exact field. Crosses: interpolated by the SW + TS expansion from power samples.**

## 6. Conclusions

Efficient, i.e., fast and accurate, sampling algorithms of central type, which allow the interpolation of electromagnetic fields over a cylindrical surface from a minimum number of samples, have been proposed.

These series are practically optimal since, for a given number of retained samples, they give rise to a truncation error essentially coincident with that relevant to the unmanageable optimal ones. Different combinations of the sampling weight functions along $z$ and along $\phi$ have been proposed and thoroughly compared by evaluating the corresponding actual reconstruction errors. The theoretical upper bounds for the truncation error relevant to the various choices have been also derived.

The accuracy of these representations has been clearly evidenced by the reported pattern reconstruction examples for both the cases of interpolation from field or power samples.

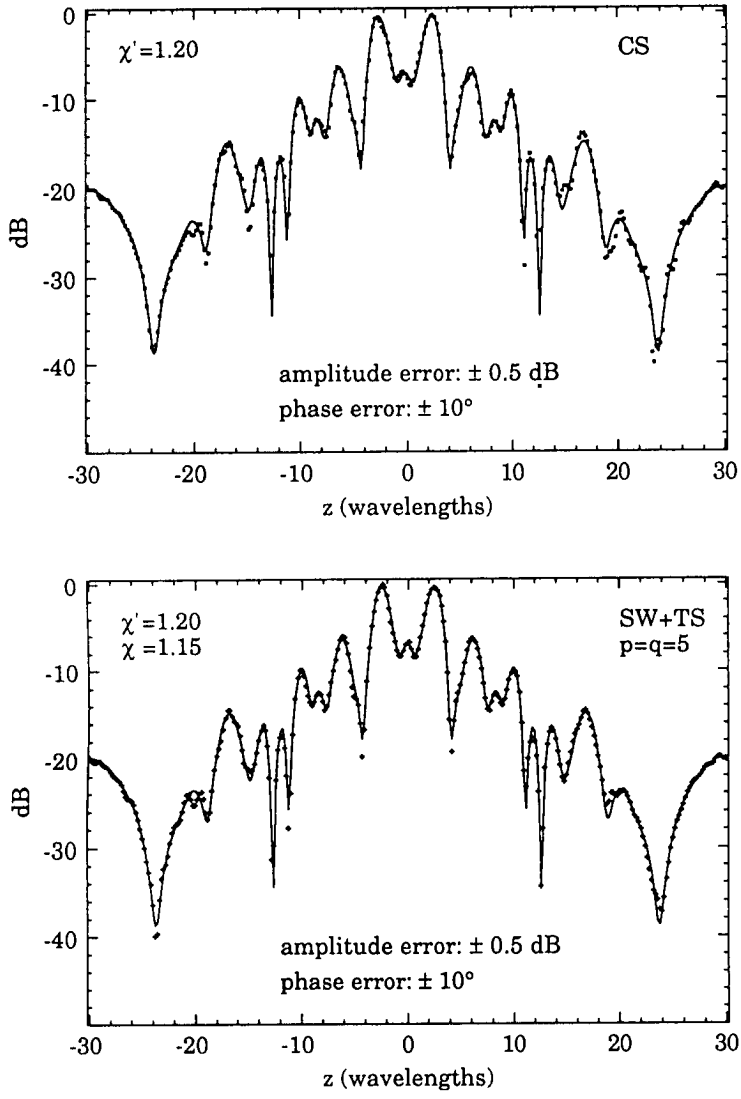


**Figure 10. Amplitude of the field $z$-component on a cylinder generatrix at $\phi = 90°$. Solid line: exact field. Squares: interpolated by the CS expansion from error affected samples. Crosses: interpolated by the SW + TS expansion from error affected samples.**

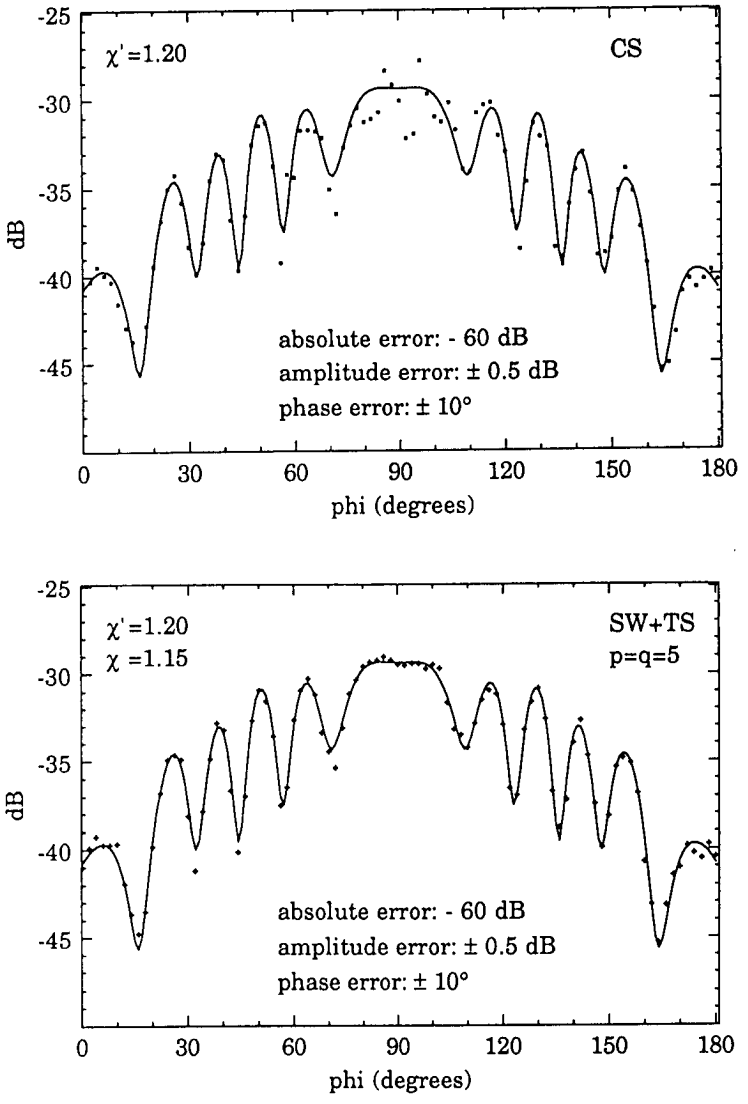


**Figure 11. Amplitude of the field $z$-component on a cylinder ring at $z = 26\lambda$. Solid line: exact field. Squares: interpolated by the CS expansion from error affected samples. Crosses: interpolated by the SW + TS expansion from error affected samples.**

Finally, numerical tests have proved their stability with respect to both absolute and relative errors in the data, showing that these expansions are remarkably more stable than the CS one.

## Appendix: The Truncation Error Bounds

In this Appendix we derive two different upper bounds for the truncation error introduced by using the expansion (17), proposed in Section 3, for the reconstruction of the electromagnetic fields over a cylindrical surface.

To this end, it is convenient to rewrite the interpolation formula (17) in the following symbolic representation:

$$\widetilde{F}(s,\phi) = \sum_{(n,m)\in I} H_n A_m F_{nm} \tag{28}$$

where $I = I_q \times I_q$ is the set of indexes of the $2q \times 2p$ samples centred on the output point $(s,\phi)$, $F_{nm} = F(s_n,\phi_{n,m})$, $H_n = H_n(s) = \Psi(s - s_n)\mathrm{sinc}[(\chi w(s-s_n)]$ and $A_m = A_m(\phi) = \Phi(\phi-\phi_{n,m})D_{M_n'}(\phi-\phi_{n,m})$.

Obviously, if the bandlimitation property is satisfied, expansion (28), by retaining all samples, allows us to obtain an exact representation of $F(s,\phi)$. Accordingly, we get

$$F(s,\phi) = \sum_{n,m} H_n A_m F_{nm} \tag{29}$$

The truncation error expression then becomes

$$\begin{aligned}\varepsilon_{pq} &= \sup|\widetilde{F} - F| \\ &= \sup\left|\sum_{(n,m)\notin I} H_n A_m F_{nm}\right| \\ &= \sup\left|\sum_{n\notin I_q,\, m} H_n A_m F_{nm} + \sum_{n\in I_q,\, m\notin I_p} H_n A_m F_{nm}\right| \end{aligned} \tag{30}$$

where the sup is evaluated for $0 \le s - s_n \le \Delta s$ and $0 \le \phi - \phi_{m_0} \le \Delta\phi$. The first term on the right-hand side of (30), can be rewritten as follows

$$\sum_{n\notin I_q,\, m} H_n A_m F_{nm} = \sum_{n\notin I_q} H_n(s) \sum_{m=-M_n'}^{M_n'} A_m(\phi)\, F_{nm}$$

$$= \sum_{n \notin I_q} H_n(s)\, F(s_n, \phi) \tag{31}$$

whereas, the second one becomes

$$\sum_{n \in I_q,\, m \notin I_p} H_n A_m F_{nm} = \sum_{n,\, m \notin I_p} H_n A_m F_{nm} - \sum_{n \notin I_q,\, m \notin I_p} H_n A_m F_{nm} \tag{32}$$

Since the left-hand side of (32) is independent from the distribution of the samples with $n \notin I_q$, it can be assumed that, if the samples are uniformly distributed in $I_q$, they are fictitiously distributed, with the same constant density, also outside $I_q$.

Accordingly, the $n$ and $m$ summations in the first term on the right-hand side of (32) can be inverted, and so:

$$\sum_{n,\, m \notin I_p} H_n A_m F_{nm} = \sum_{m \notin I_p} A_m(\phi) \sum_{n=-\infty}^{\infty} H_n(s)\, F_{nm}$$

$$= \sum_{m \notin I_p} A_m(\phi)\, F(s, \phi_m) \tag{33}$$

On the other hand:

$$\sum_{n \notin I_q,\, m \notin I_p} H_n A_m F_{nm} = \sum_{n \notin I_q} H_n(s) \sum_{m \notin I_p} A_m(\phi)\, F_{nm} \tag{34}$$

And so, for the truncation error, we have:

$$\varepsilon_{pq} = \sup \Bigg| \sum_{n \notin I_q} H_n(s)\, F(s_n, \phi) + \sum_{m \notin I_p} A_m(\phi)\, F(s, \phi_m) - \sum_{n \notin I_q} H_n(s) \sum_{m \notin I_p} A_m(\phi)\, F_{nm} \Bigg| \tag{35}$$

hence, by majoring, we get:

$$\varepsilon_{pq} \leq \sup \Bigg| \sum_{n \notin I_q} H_n(s)\, F(s_n, \phi) \Bigg| + \sup \Bigg| \sum_{m \notin I_p} A_m(\phi)\, F(s, \phi_m) \Bigg| + \sup \Bigg| \sum_{n \notin I_q} H_n(s) \sum_{m \notin I_p} A_m(\phi)\, F_{nm} \Bigg| \tag{36}$$

The first two terms on the right-hand side of (36) are the one-dimensional truncation errors relevant to a rectilinear and circular domain, respectively and, therefore, we get:

$$\varepsilon_q = \sup\left|\sum_{n \notin I_q} H_n(s)\, F(s_n, \phi)\right| \leq \sup_{0 \leq \phi - \phi_{m_0} \leq \Delta\phi} \delta_q \left(\sup_s |F(s, \phi)|\right)$$

$$\leq \delta_q \sup_{s,\phi} |F(s, \phi)| = \delta_q \, \| F \| \tag{37}$$

$$\varepsilon_p = \sup\left|\sum_{m \notin I_p} A_m(\phi)\, F(s, \phi_m)\right| \leq \sup_{0 \leq s - s_{n_0} \leq \Delta s} \delta_p \left(\sup_\phi |F(s, \phi)|\right)$$

$$\leq \delta_p \sup_{s,\phi} |F(s, \phi)| = \delta_p \, \| F \| \tag{38}$$

where $\delta_p$ and $\delta_q$ are the one-dimensional maximum normalized errors (see Section 2).

With reference to the last term of (36), it can be majored as follows:

$$\sup\left|\sum_{n \notin I_q} H_n(s) \sum_{m \notin I_p} A_m(\phi)\, F_{nm}\right|$$

$$= \sup\left|\sum_{n \notin I_q} H_n(s) \left(\sum_{m \notin I_p} A_m(\phi)\, F(s_n, \phi_m)\right)\right|$$

$$\leq \delta_q \sup_s \left|\sum_{m \notin I_p} A_m(\phi)\, F(s, \phi_m)\right|$$

$$\leq \delta_q \sup_s \left(\delta_p \sup_\phi |F(s, \phi)|\right)$$

$$\leq \delta_q \delta_p \, \| F \| \tag{39}$$

According to (36)–(39), we obtain:

$$\varepsilon_{pq} \leq \delta_q \, \| F \| + \delta_p \, \| F \| + \delta_q \delta_p \, \| F \| \tag{40}$$

i.e.:

$$\delta_{pq} \leq (1+\delta_p)(1+\delta_q) - 1 \tag{41}$$

Let us now derive a different upper bound by using the square norm. By applying the Schwartz inequality to (30), we have:

$$|\varepsilon_{pq}|^2 \leq \sup\left\{ \sum_{(n,m)\notin I} |H_n A_m|^2 \sum_{(n,m)\notin I} |F_{nm}|^2 \right\} \tag{42}$$

where it is possible to write:

$$\sum_{(n,m)\notin I} |H_n A_m|^2 = \sum_{n\notin I_q, m} |H_n A_m|^2 + \sum_{n\in I_q, m\notin I_p} |H_n A_m|^2 \tag{43}$$

In this last expression, with reference to the first term on the right hand side, we obtain

$$\begin{aligned} \sum_{n\notin I_q, m} |H_n A_m|^2 &= \sum_{n\notin I_q} \left[ |H_n(s)|^2 \sum_{m=-M_n'}^{M_n'} |A_m(\phi)|^2 \right] \\ &\leq \sum_{n\notin I_q} \left[ |H_n(s)|^2 \sum_{m=-M_n'}^{M_n'} \left| D_{M_n'}(\phi - \phi_{n,m}) \right|^2 \right] \\ &= \sum_{n\notin I_q} |H_n(s)|^2 \end{aligned} \tag{44}$$

while, by assuming that $M_n'$ does not change for all $n \in I_q$, for the latter

$$\begin{aligned} \sum_{n\in I_q, m\notin I_p} |H_n A_m|^2 &= \left[ \sum_{n\in I_q} |H_n(s)|^2 \right] \left[ \sum_{m\notin I_p} |A_m(\phi)|^2 \right] \\ &\leq \sum_{n=-\infty}^{\infty} |\operatorname{sinc}(s - s_n)|^2 \sum_{m\notin I_p} |A_m(\phi)|^2 \\ &= \sum_{m\notin I_p} |A_m(\phi)|^2 \end{aligned} \tag{45}$$

because

$$\sum_{m=-M_n'}^{M_n'} \left| D_{M_n'}(\phi - \phi_{n,m}) \right|^2 = 1 \tag{46}$$

and

$$\sum_{n=-\infty}^{\infty} |\operatorname{sinc}(s - s_n)|^2 = 1 \tag{47}$$

Therefore, according to (43)–(45), (42) becomes:

$$|\varepsilon_{pq}|^2 \leq \sup \left[ \sum_{n \notin I_q} |H_n(s)|^2 + \sum_{m \notin I_p} |A_m(\phi)|^2 \right] \cdot \sum_{(n,m) \notin I} |F_{nm}|^2 \tag{48}$$

which can be further majored by taking into account that

$$\begin{aligned} \sum_{(n,m) \notin I} |F_{nm}|^2 &\leq \sum_{n,m} |F_{nm}|^2 \\ &= \sum_{n=-\infty}^{\infty} \sum_{m=-M_n'}^{M_n'} |F_{nm}|^2 \\ &= \sum_{n=-\infty}^{\infty} \frac{1}{\Delta\phi_n} \int_0^{2\pi} |F(s_n, \phi)|^2 \, d\phi \end{aligned} \tag{49}$$

wherein

$$\Delta\phi_n \cong \frac{\pi}{\chi\chi'\beta a \sin\theta_n} \tag{50}$$

Now, being $\cot\theta_n = s_n$, we have

$$\sin\theta_n = \frac{1}{\sqrt{1 + s_n^2}} \tag{51}$$

that, substituted in (50), gives:

$$\Delta\phi_n \cong \frac{\pi\sqrt{1 + s_n^2}}{\chi\chi'\beta a} \tag{52}$$

Accordingly, the Eq. (49) becomes

$$\sum_{(n,m)\notin I} |F_{nm}|^2 \leq \left(\frac{\chi\chi'\beta a}{\pi}\right) \sum_{n=-\infty}^{\infty} \frac{1}{\sqrt{1+s_n^2}} \int_0^{2\pi} |F(s_n,\phi)|^2 \, d\phi$$

$$\cong \left(\frac{\chi\chi'\beta a}{\pi}\right) \frac{1}{\Delta s} \int_{-\infty}^{\infty} \int_0^{2\pi} \frac{|F(s,\phi)|^2}{\sqrt{1+s^2}} \, ds \, d\phi = \left(\frac{\chi\chi'\beta a}{\pi}\right)^2 \| F \|_{2w}^2 \tag{53}$$

where $\| F \|_{2w}$ is the weighted square norm of $F$ with weight $1/\sqrt{1+s^2}$.

It is convenient to consider a normalized "equivalent" height $H$, such that

$$2\pi H \| F \|^2 = \| F \|_{2w}^2 \tag{54}$$

and so, the inequality (53) becomes

$$\sum_{(n,m)\notin I} |F_{nm}|^2 \leq 2\pi H \left(\frac{\chi\chi'\beta a}{\pi}\right)^2 \| F \|^2 \tag{55}$$

which substituted in (48) gives

$$|\varepsilon_{pq}|^2 < 2\pi H \, (\bar{\delta}_q^2 + \bar{\delta}_p^2) \left(\frac{\chi\chi' 2a}{\lambda}\right)^2 \| F \|^2 \tag{56}$$

In this latter, $\bar{\delta}_q^2$ and $\bar{\delta}_p^2$ are the maxima of the bracketed terms in (48), which, due to the symmetry of the functions, occur at the middle points of the sampling intervals, i.e.:

$$\bar{\delta}_q^2 = \sum_{n\notin I_q} |H_n(\Delta s/2)|^2 \tag{57}$$

$$\bar{\delta}_p^2 = \sum_{m\notin I_p} |A_m(\Delta\phi/2)|^2 \tag{58}$$

And so, we finally obtain the following alternative upper bound for the normalized truncation error

$$\delta_{pq} = \frac{|\varepsilon_{pq}|}{\| F \|} \leq \sqrt{2\pi H}\, \chi\chi' \left(\frac{2a}{\lambda}\right) \sqrt{\bar{\delta}_p^2 + \bar{\delta}_q^2} \tag{59}$$

The upper bounds for $\bar{\delta}_p^2$ and $\bar{\delta}_q^2$ are reported, for reader's convenience, in Section 3.

## References


1. Bucci, O. M., G. Franceschetti, G. D'Elia, C. Gennarelli, G. Mazzarella, R. Pierri, G. Leone, and G. Schirinzi, "Application of sampling techniques to near-field-far-field transformation," *ESTEC Contract n. 5709/83/NL/GH, Final Report,* December 1986.
2. Bucci, O. M., and C. Gennarelli, "Use of sampling expansions in near-field-far-field transformations: the cylindrical case," *IEEE Trans. Antennas Propagat.,* Vol. AP-36, 830–835, 1988.
3. Bucci, O. M., C. Gennarelli, and C. Savarese, "Near-field-far-field transformation by cardinal series interpolation of plane-polar measurements," *Annali Facoltá Scienze Nautiche,* Vol. LVI, I.U.N., 151–170, Napoli, Italy, 1988.
4. Bucci, O. M., C. Gennarelli, and C. Savarese, "A new fast and accurate near-field-far-field transformation with plane-polar scanning," *Proc. ICEAA,* 313–316, Torino, Italy, 1989.
5. Bucci, O. M., C. Gennarelli, and C. Savarese, "Fast and accurate near-field-far-field transformation by sampling interpolation of plane-polar measurements," *IEEE Trans. Antennas Propagat.,* Vol. AP-39, 48–55, January, 1991.
6. Bucci, O. M., G. Franceschetti, and G. D'Elia, "Fast analysis of large antennas. A new computational philosophy," *IEEE Trans. Antennas Propagat.,* Vol. AP-28, 306–310, 1980.
7. Bucci, O. M., G. D'Elia, and G. Franceschetti, "Computation of radiation from reflector antennas: an optimal strategy," *Alta Freq.,* Vol. 49, 390–399, 1980.
8. Bucci, O. M., and G. Di Massa, "Exact sampling approach for reflector antenna analysis," *IEEE Trans. Antennas Propagat.,* Vol. AP-32, 1259–1261, 1984.
9. Rahmat-Samii, Y., and R. L. T. Cheung, "Nonuniform sampling techniques for antenna applications," *IEEE Trans. Antennas Propagat.,* Vol. AP-35, 268–279, 1987.

10. Bucci, O. M., C. Gennarelli, and C. Savarese, "Optimal interpolation of radiated fields over a sphere," *IEEE Trans. Antennas Propagat.*, Vol. AP-39, 1633–1643, 1991.
11. Bucci, O. M., and G. Franceschetti, "On the spatial bandwidth of scattered fields," *IEEE Trans. on Antennas Propagat.*, Vol. AP-35, 1445–1455, 1987.
12. Bucci, O. M., and G. Di Massa, "The truncation error in the application of sampling series to electromagnetic problems," *IEEE Trans. Antennas Propagat.*, Vol. AP-36, 941–949, 1988.
13. Bucci, O. M., C. Gennarelli, C. Savarese, and F. Falcinelli, "Optimal interpolation of radiated fields over a plane from plane-polar samples," *Annali Facoltá di Scienze Nautiche.*, supplement to Vol. LX, 1–35, Napoli, Italy, 1993.
14. Stark, H., J. W. Woods, I. Paul, and R. Hingorani, "Direct Fourier reconstruction in computer tomography," *IEEE Trans. Acoust. Speech, Signal Processing,* Vol. ASSP-29, 237–245, 1981.
15. Peng, H., and H. Stark, "Direct Fourier reconstruction in fan-beam tomography," *IEEE Trans. Med. Imaging,* Vol. MI-6, 209–219, 1987.
16. Yudilevich, E., and H. Stark, "Interpolation from samples on a linear spiral scan," *IEEE Trans. Med. Imaging,* Vol. MI-6, 193–200, 1987.
17. Grue, K. E., "Optimal reconstruction of bandlimited bounded signals," *IEEE Trans. Inf. Theory,* Vol. IT-31, 594–600, 1985.
18. Knab, J. K., "Interpolation of bandlimited functions using the approximate prolate series," *IEEE Trans. Inf. Theory,* Vol. IT-25, 717–720, 1979.
19. Knab, J. K., "The sampling window," *IEEE Trans. Inf. Theory,* Vol. IT-29, 157–159, 1983.
20. Bucci, O. M., C. Gennarelli, and C. Savarese, "Interpolation of radiated fields over a sphere," *Annali Facoltá Scienze Nautiche,* Vol. LVIII, I.U.N., Napoli, Italy, 1990.